

Laminar Separating Flow over Backsteps and Cavities

Part II: Cavities

S. N. Sinha,* A. K. Gupta,† and M. M. Oberai‡
Indian Institute of Technology, Kanpur, India

Data on flow over backsteps and cavities for the laminar case are very scant. The present paper reports the results of an experimental investigation carried out at a wind speed of 1.8 m/s past eight rectangular cavities of depth 0.625, 1.25, and 2.5 cm and depth-to-width ratios h/b in the range 0.035-2.5; the separating boundary layer in all cases was laminar and was of thickness 1.4 cm. The Reynolds numbers, based on the cavity depth, were 662, 1324, and 2648. Results of smoke flow visualization and static pressure and hot-wire measurements show that as in the case of turbulent flows, cavities can be classified as closed, shallow open, and open depending on the range of the value of the ratio h/b . The mean velocity profiles in the free shear region show self-similarity and the flow in the recirculating region of the shallow open cavity appears to have the character of a wall jet in the reverse direction superimposed on a forward-moving free shear layer. Typical development of streamwise mean velocity profile and intensity of fluctuations are also presented.

Nomenclature

b	= width of the rectangular cavity
C_p	= pressure coefficient = $(p - p_\infty)/(\frac{1}{2}\rho U_\infty^2)$
h	= depth of the cavity
p	= static pressure
Re_b	= $U_\infty b/\nu$
Re_h	= $U_\infty h/\nu$
u'	= x component of fluctuating velocity
U	= x component of mean velocity
U_m	= local maximum value of U
U_r	= x component of reverse flow velocity
U_{rm}	= local maximum value of U_r
x	= coordinate along the cavity floor with origin at the separation edge
x_t	= transition location from the separation edge
y	= coordinate normal to the cavity floor with origin at the separation edge
$y_{1/2}$	= y location at which $U = \frac{1}{2}U_m$
$y_{r/2}$	= y location at which $U_r = \frac{1}{2}U_{rm}$
δ	= boundary-layer thickness
δ^*	= displacement thickness
Θ	= momentum thickness = $\int_0^\infty (U/U_m)[1 - (U/U_m)]dy$
ν	= kinematic viscosity of air = $1.7 \times 10^{-5} \text{ m}^2/\text{s}$

Subscripts

∞	= freestream condition at reference point
h	= at separation edge

Introduction

FLOW past backsteps and cavities is an important example of separated flows. Little progress in the understanding of the characteristics and mechanics of such flows has been reported in the literature. Analytical and numerical studies have not been very helpful in predicting or explaining the mechanics of such flows. Also, the experimental data for these flows are very scant, especially for the laminar case. An

experimental investigation was undertaken to collect data on various characteristics of flows past backsteps and rectangular cavities. The results for the backsteps were reported in Part I by Sinha et al.¹ and results for the cavities are reported herein.

Brief Literature Survey of Flow Past Cavities

A number of experimental investigations of flow past cavities have been reported but most of them pertain to high Reynolds number regime in which the separation at the cavity wall is turbulent. For the case of low Reynolds number, there are several numerical studies, e.g., by Kawaguti,² Mills,³ Burggraf,⁴ Pan and Acrivos,⁵ Nallaswamy and Prasad,⁶ and Bozeman and Dalton.⁷ However, due to mathematical difficulties, the boundary condition at the free surface had to be chosen so as to necessitate the assumption that the flow is induced by a top moving wall. Thus the interaction between the recirculating flow inside the cavity and the external flow (which is very important in real situations) did not form a part of the above-mentioned numerical studies. On the experimental side, Sarohia⁸ has investigated laminar separating flow over axisymmetric rectangular cavities and reported that, as in the turbulent separation case, the value of the depth-to-width ratio h/b can be used to classify a cavity as "closed" or "open" according to whether the separating shear layer reattaches on the floor or on the downstream face of the cavity. The demarcating value of the ratio h/b was found to lie in the range of 0.11-0.14. He also observed a similarity in the velocity profiles of the laminar separating shear layer.

Scope of the Present Work

The present paper reports results of an experimental investigation of laminar parallel (the separating layer leaves the surface at zero angle) separating flow over two-dimensional rectangular cavities covering a range of depths h and ratios h/b . The values of δ_h/h for different cases were 2.24, 1.12, and 0.56. Reynolds number Re_b covered the range of 1060-19,580. The flow details were studied through a smoke visualization technique, static pressure measurements on the cavity walls, and hot-wire anemometry for streamwise mean velocity profiles and intensity of fluctuations.

The objective of the present study is limited to reporting the data obtained. Considerable additional data are needed to form the basis for an effort to understand and explain the various mechanisms that characterize such flows.

Received Feb. 23, 1981; revision received Aug. 20, 1981. Copyright © American Institute of Aeronautics and Astronautics, Inc., 1981. All rights reserved.

*Q.I.P. Fellow; presently at Dept. of Mechanical Engineering, Bihar College of Engineering, Patna, India.

†Professor, Dept. of Aeronautical Engineering.

‡Professor, Dept. of Mechanical Engineering.

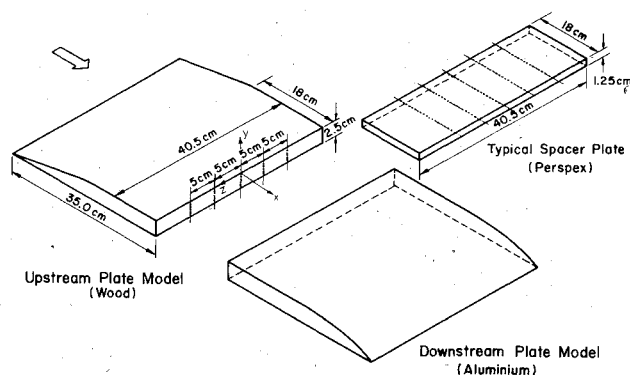


Fig. 1 The cavity models.

Experiments

The experimental setup and techniques were the same as described in Part I of this investigation.¹ Cavity models were formed on the floor of the test section spanning the test section width of 40.5 cm (as shown in Fig. 1) by a combination of a common half-wedge type of upstream plate model and an appropriate downstream plate model with a spacer plate in between. For checking the two-dimensionality of flow, five rows of static pressure orifices of 1 mm diam were provided along the periphery of each model as shown in Fig. 1. In all, eight different rectangular cavity flows were studied. Table 1 presents the summary of geometrical and dynamical parameters, the cavity code, and classification.

The tests were conducted in an open-circuit suction-type low-speed wind tunnel with a test section 40.5 cm wide, 30.5 cm high, and 100 cm long. The tunnel freestream turbulence level was about 0.15% at a wind speed of 1.8 m/s. The blockage ratios for the cavity depths of 0.625, 1.25, and 2.5 cm were 2.05, 4.1, and 8.2%, respectively. The incoming flow condition was determined by measuring the mean streamwise velocity profiles with the help of a single hot-wire probe at three streamwise locations upstream of the separation edge ($x = -10.38$, -5.33 , and -0.15 cm). These velocity profiles are shown in Fig. 2. The solid lines passing through the data points represent the results of the sixth-degree polynomial fits obtained by the method of least square error. Different integrated parameters such as δ^* and Θ were calculated for each of the three velocity profiles. At $x = -0.15$ cm, the characteristics of the laminar boundary-layer velocity profile were: $\delta = 1.4$ cm, $\delta^* = 0.406$ cm, $\Theta = 0.177$ cm, and $H = \delta^*/\Theta = 2.29$.

The smoke flow visualization technique was employed to obtain the overall qualitative picture of the complicated,

recirculating-type flow with corner regions which are characteristic of rectangular cavity flows. Static pressure measurements were carried out in the "clean" configuration of the cavity models, i.e., without any probe interference, to determine pressure profiles characterizing different types of cavity flows. An electronic manometer (Barocel 1014) with a pressure cell of 0.7 kg/cm^2 range was employed for this purpose. The reference pressure and velocity used for computing C_p were recorded at a point 7 cm upstream of the separation line and 15 cm above the test section floor.

The hot-wire anemometry technique was employed for measurement of streamwise mean velocity profile and intensity of fluctuation. The single hot-wire probe consisted of 2.8 cm long prongs (as the deepest cavity had $h = 2.5$ cm, the stem of the probe never entered the cavity) made of hypodermic tubing of 1 mm diam; the spacing between the centers of the prongs was 2 mm. The stem was 76 cm long with 6 mm diam; it tapered down to 4 mm diam in the lower 10 cm portion adjacent to the prongs. Thus, the blockage ratio of the prongs in the cavity region was 0.5% and that of the stem in the test section region was less than 1.5%. Our experience has shown that with such low blockage ratios the interference to the flow is negligible. The sensor was made from Wollaston platinum wire of $7.5 \mu\text{m}$ diameter. As the effective length of the sensor was 1 mm, the aspect ratio was about 125. In view of the low wind velocities a comparatively low overheat value of 1.45 was employed. The normal orientation of the hot-wire axis was parallel to the cavity edge from which the flow separated. DISA 55A01 constant temperature hot-wire anemometer in conjunction with a Fluke 830 DA digital dc voltmeter was used for measurements. For calibration in the low-velocity region a fourth-degree speed-voltage curve was fitted using the least square technique. For further details of calibration and calculation of mean velocities and intensity of fluctuation, one may refer to Refs. 1 and 9.

The hot-wire anemometry technique has some merits, e.g., fine space resolution of almost a point measurement, minimal sensor interference to the flow, fast frequency response for the intensity of fluctuations, and high resolution electrical output. However, a single hot wire is insensitive to flow direction in pitch and therefore cannot detect the reverse velocity direction. For the same reason, mean streamwise velocity measurements are not very reliable near the corners where the inclination of the mean flow streamlines to the cavity floor is significant. Also, the hot-wire anemometer gives accurate values of the intensity of fluctuations only when the fluctuations are small compared to the mean velocity. But as the more sophisticated instrumentation such

Table 1 Code and summary for cavities^a

Serial No.	Code	h depth, cm	b width, cm	Re_h	Re_b	h/b	δ_h/h	x_t/h	Classification	Flow configuration ^b
1	C-0.625-0.104	0.625	6	662	6,333	0.104	2.22	* ^c	Shallow, open	
2	C-0.625-0.035	0.625	18	662	19,000	0.035	2.22	*	Shallow, closed	
3	C-1.25-0.139	1.25	9	1324	9,500	0.139	1.1	*	Shallow, open	
4	C-1.25-0.069	1.25	18	1324	19,000	0.069	1.1	7.5	Shallow, closed	
5	C-2.5-2.5	2.5	1	2648	1,058	2.5	0.56	*	Deep	
6	C-2.5-1.0	2.5	2.5	2648	2,648	1.0	0.56	*	Open	
7	C-2.5-0.5	2.5	5	2648	5,296	0.5	0.56	*	Open	
8	C-2.5-0.139	2.5	18	2648	19,000	0.139	0.56	6.0	Open	

^aIncoming flow conditions, $U_\infty = 1.8 \text{ m/s}$ and $\delta_h = 1.4 \text{ cm}$, are same for all cavity flows. ^bL = laminar, T = turbulent. ^c* indicates that the transition to turbulence has not taken place within the entire cavity width b .

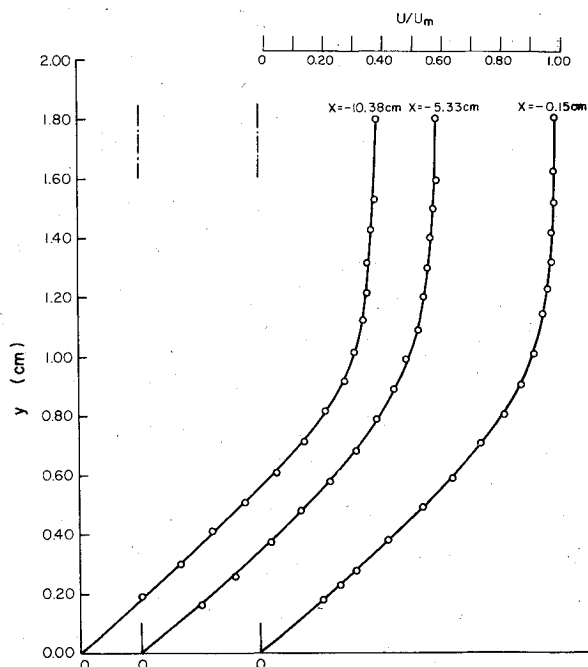


Fig. 2 Velocity profiles at different locations ahead of separation ($U_\infty = 180$ cm/s).

as the laser anemometer was not available to the authors and the detailed measurements of the mean velocity and intensity of fluctuations have not previously been reported in the literature, it is hoped that the present results of the hot-wire measurements will be found valuable at least for getting a picture of the qualitative trends. Portions of velocity profiles falling in the zones of uncertainty are shown in dotted lines in the corresponding figures. Smoke flow patterns have been used to ascertain the flow direction near the floor and have been found generally useful in determining the zones of uncertainty. Further discussion on the limitations of the present data imposed by the available instrumentation is given by Sinha.⁹

Results and Discussion

Flow Pattern

Smoke patterns for laminar separating flow over the eight cavities suggest the four types of flow patterns described below. The criterion of transition to turbulence of the separating laminar shear layer is based on these smoke flow patterns, and is therefore qualitative in nature. The x station at which the parallel, sharply distinct smoke streak breaks up into a diffuse random smoking bubbly pattern is identified as the transition location.

1) Shallow, closed cavity flow for $h/b \leq 0.1$ was characterized by two separation bubbles, one formed due to the upstream face and the other formed due to the downstream face of the cavity. In this category, the flow in C-0.625-0.035 was entirely laminar while the bubble formed near the downstream face of C-1.25-0.069 appeared to be turbulent.

2) Shallow, open cavity flow for $0.1 \leq h/b \leq 0.5$ was characterized by a single elongated eddy. In this category, the flow in both C-0.625-0.104 and C-1.25-0.139 was entirely laminar. In both cases the eddy center was located significantly downstream of the geometric center of the cavity. In the case of C-2.5-0.139 the flow was turbulent near the downstream face. A comparison of smoke patterns for backsteps of heights 1.25 and 2.5 cm (Sinha et al.¹) with the corresponding smoke patterns of C-1.25-0.139 and C-2.5-0.139 showed that the presence of the downstream face in cavities delayed transition of the separating shear layer from $x = 4.5h$ (backstep) to $7.5h$ (cavity) for $h = 1.25$ cm and from $x = 2h$ (backstep) to $6h$ (cavity) for $h = 2.5$ cm.

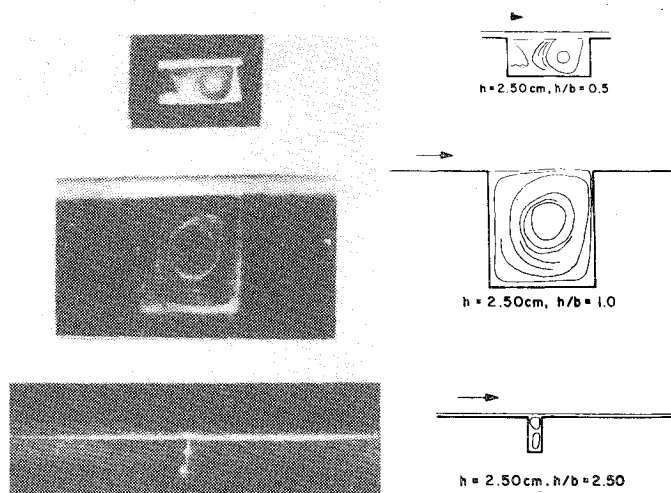


Fig. 3 Smoke patterns and schematic representation for flow over open cavities ($h/b = 0.5, 1.0$, and 2.5 , $h = 2.5$ cm).

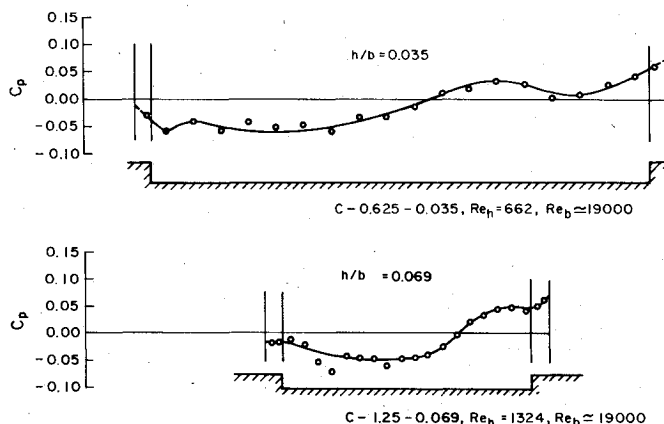


Fig. 4 Pressure distributions along the walls of the closed cavities C-0.625-0.035 and C-1.25-0.069.

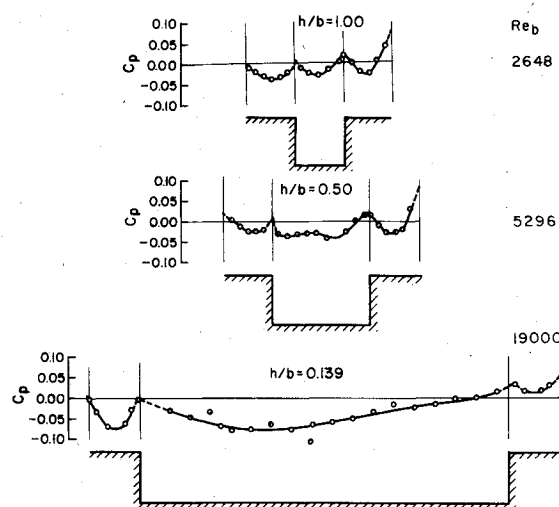


Fig. 5 Pressure distributions along the walls of the open cavities C-2.5-0.139, C-2.5-0.5, and C-2.5-1.0.

3) Open cavity flows for $0.5 \leq h/b \leq 1.5$ were characterized by a single laminar eddy (Fig. 3) along with a secondary separation bubble in the upstream corner. For C-2.5-0.5 the vortex center was located at $x/b = 0.66$, $y/h = -0.47$, and the secondary bubble occupied about 30% of the cavity region.

Fig. 6 Mean velocity and fluctuation intensity profiles for the open cavity C-1.25-0.139 ($U_\infty = 1.95$ m/s, $Re_h = 1434$, and $Re_b = 10,320$).

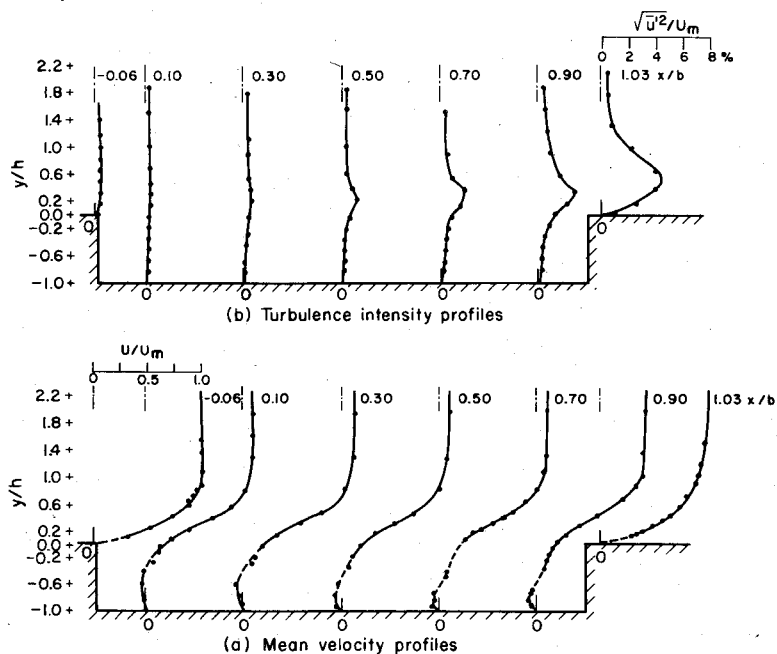


Fig. 7 Mean velocity and fluctuation intensity profiles for the open cavity C-2.5-0.139 ($U_\infty = 1.85$ m/s, $Re_h = 2720$, and $Re_b = 19,580$).

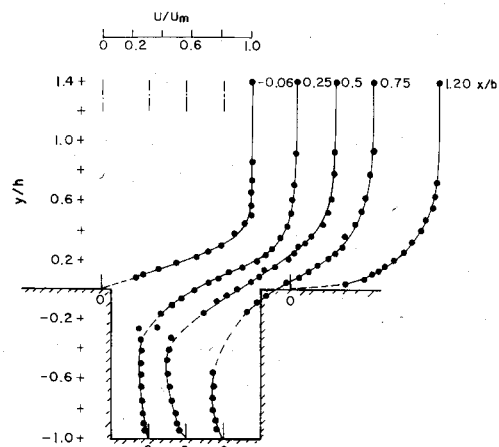
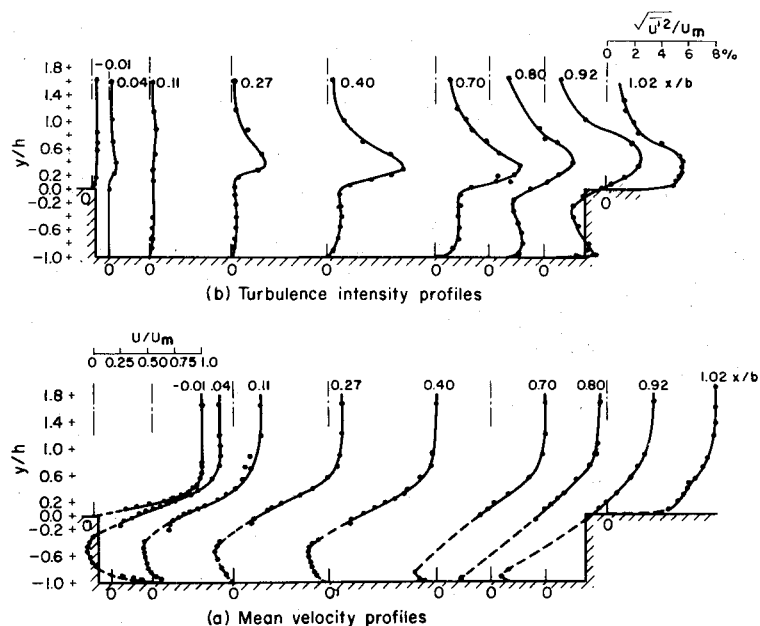


Fig. 8 Mean velocity profiles for the square cavity C-2.5-1.0 ($U_\infty = 1.85$ m/s and $Re_h = Re_b = 2720$).

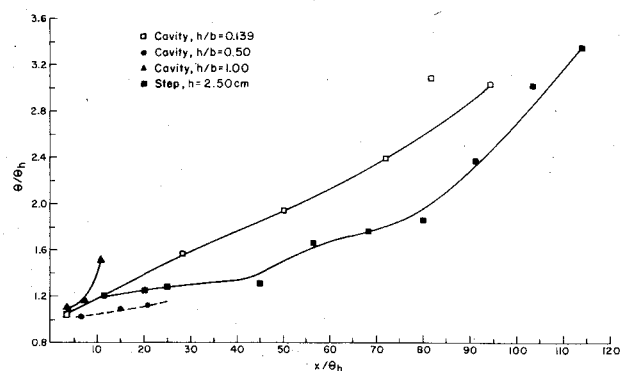


Fig. 9 Variation of laminar separated shear layer θ with downstream distance for cavities ($h = 2.5$ cm).

These features are in agreement with the photographic data of Hardin and Mason.¹⁰ For the square cavity C-2.5-1.0 the vortex center was located at $x/b \approx 0.54$, $y/h \approx -0.46$.

4) Deep cavity for $h/b \geq 1.5$ was characterized by more than one laminar vortex rolling one above the other. Figure 3 shows two laminar vortices for C-2.5-2.5.

Static Pressure Measurements

The data obtained from five rows of pressure taps in different cavities showed that the flow in all cases was two-dimensional. The static pressure distribution for closed cavities C-0.625-0.035 and C-1.25-0.069 (Fig. 4) appears to be a combination of pressure distribution on a backstep followed by one due to a forward-facing step. For the open cavities, flow was dominated by a single laminar eddy. The pressure distribution (Fig. 5) is characterized by negative pressure over most of the cavity floor followed by a small pressure recovery in the downstream face region.

Mean Velocity and Velocity Fluctuations

Typical development of mean velocity profiles and intensity of fluctuations for cavities C-1.25-0.139, C-2.5-0.139, and C-2.5-1.0 are shown in Figs. 6, 7, and 8, respectively. Following are the salient features of these profiles. The mean flow in the

open cavity C-1.25-0.139 appears to be entirely laminar, while the intensity of fluctuations (Fig. 6) indicates that the separated shear region is undergoing transition. On the other hand, the flow in the open cavity C-2.5-0.139 starts out as laminar and becomes turbulent near $x/b \approx 1.0$. Figure 7b shows two peaks, one near $y \approx 0.2h$ and the other close to the cavity floor for $x/b \geq 0.7$, indicating the onset of turbulence. For the square cavity the mean flow profiles for three x stations inside the cavity are shown in Fig. 8. Inside the square cavity the intensity of fluctuations was less than 1% everywhere. Similar data for other cavities are presented by Sinha.⁹

Typical plots for streamwise variation of momentum thickness Θ of separated shear layer for rectangular cavities of depth 2.5 cm are shown in Fig. 9. Corresponding data for the backstep of $h = 2.5$ cm are also shown. It appears that the growth rate of Θ for the cavity C-2.5-0.139 is higher than that of C-2.5-1.0. More elaborate experiments designed to study this aspect are needed to draw a definite conclusion.

Using similarity parameters of Sato,¹¹ mean velocity profiles in the laminar separating shear region were plotted for different cavity flows. A typical plot for the open cavity C-1.25-0.139 is shown in Fig. 10. Satisfactory self-similarity characteristics are observed in the range of $0 < x/b < 1$ as long as separating shear layer remains laminar.

The allure of the mean velocity profiles for C-1.25-0.139 shown in Fig. 7 suggests that the reverse flow has qualitative features similar to those of a laminar wall jet. Accordingly, these data are plotted in wall jet coordinates U/U_m vs $y/y_{r/2}$ in Fig. 11. Considerable scatter is observed near $y/y_{r/2} \approx 0$ and 1.0 due to experimental uncertainty in measurements of low velocities. However, the self-similarity for reverse flow looks promising and calls for further investigation.

Conclusion

The nature of flow in a rectangular cavity with laminar separation is controlled mainly by the h/b ratio; $h/b \approx 0.1$ is the demarcating value between closed and open cavities, $h/b \geq 0.1$ resulting in open cavities. The ratio δ_h/h also affects the flow, but in a manner which is not quite clear at present. As long as the separating shear layer remains laminar, the mean velocity profiles exhibit self-similarity. For open cavities with laminar flow, the reverse flow velocity profiles also show approximate self-similarity when plotted in wall jet coordinates.

Acknowledgment

The authors wish to thank K. S. Muddappa, R. Krishnamurthy, and D. K. Sarkar for assistance in the experimental program.

References

- 1 Sinha, S. N., Gupta, A. K., and Oberai, M. M., "Laminar Separating Flow Over Backsteps and Cavities, Part I: Backsteps," *AIAA Journal*, Vol. 19, Dec. 1981, pp. 1524-1530.
- 2 Kawaguti, M., "Numerical Solution of the Navier-Stokes Equation for Flow into a Two Dimensional Cavity," *Journal of the Physical Society of Japan*, Vol. 16, Nov. 1961, pp. 2307-2315.
- 3 Mills, R. D., "Numerical Solution of the Viscous Flow Equations for a Class of Closed Flows," *Journal of the Royal Aeronautical Society*, Vol. 69, Oct. 1965, pp. 714-718.

§One of the referees has suggested that it is likely that the effect of δ_h/h may relate to the quenching of turbulence in shear layers caused by wall proximity. Table 1 indicates that for a constant value of $Re_b = 19,000$, x_i/h decreases as δ_h/h decreases. The suggestion is gratefully acknowledged.

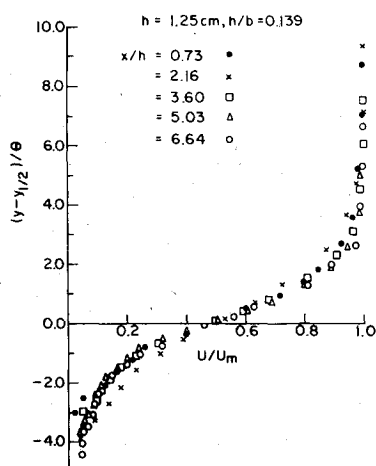


Fig. 10 Similarity of laminar separated shear layer velocity profiles for flow over open cavity C-1.25-0.139 ($Re_h = 1324$ and $Re_b = 9525$).

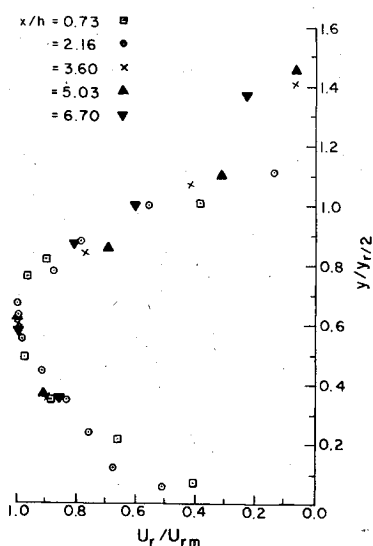


Fig. 11 Similarity in reverse flow velocity profiles for cavity C-1.25-0.139 ($Re_h = 1324$ and $Re_b = 9525$).

⁴Burggraf, O. R., "Analytical and Numerical Study of the Structure of Steady Separated Flows," *Journal of Fluid Mechanics*, Vol. 24, Jan. 1966, pp. 113-151.

⁵Pan, F. and Acrivos, A., "Steady Flow in Rectangular Cavities," *Journal of Fluid Mechanics*, Vol. 28, June 1967, pp. 643-655.

⁶Nallaswamy, M. and Prasad, K. K., "On Cavity Flow at High Reynolds Number," *Journal of Fluid Mechanics*, Vol. 79, Feb. 1977, pp. 391-414.

⁷Bozeman, J. D. and Dalton, C., "Numerical Study of Viscous Flow in a Cavity," *Journal of Computational Physics*, Vol. 12, July 1973, pp. 348-363.

⁸Sarohia, V., "Experimental Investigation of Oscillation in Flow

Over Shallow Cavities," *AIAA Journal*, Vol. 15, July 1977, pp. 984-991.

⁹Sinha, S. N., "Two Dimensional Laminar and Turbulent Separating Flows over Backward Facing Steps and Rectangular Cavities," Ph.D. Thesis, Indian Institute of Technology, Kanpur, India, 1978 (available from University Microfilms International).

¹⁰Hardin, J. G. and Mason, J. P., "Broad Band Noise Generation by a Vortex Model of Cavity Flow," *AIAA Journal*, Vol. 15, May 1977, pp. 632-637.

¹¹Sato, H., "Experimental Investigation on the Transition of Laminar Separated Layer," *Journal of the Physical Society of Japan*, Vol. 11, June 1956, pp. 702-709.

From the AIAA Progress in Astronautics and Aeronautics Series . . .

GASDYNAMICS OF DETONATIONS AND EXPLOSIONS—v. 75 and COMBUSTION IN REACTIVE SYSTEMS—v. 76

*Edited by J. Ray Bowen, University of Wisconsin,
N. Manson, Université de Poitiers,
A. K. Oppenheim, University of California,
and R. I. Soloukhin, BSSR Academy of Sciences*

The papers in Volumes 75 and 76 of this Series comprise, on a selective basis, the revised and edited manuscripts of the presentations made at the 7th International Colloquium on Gasdynamics of Explosions and Reactive Systems, held in Göttingen, Germany, in August 1979. In the general field of combustion and flames, the phenomena of explosions and detonations involve some of the most complex processes ever to challenge the combustion scientist or gasdynamicist, simply for the reason that *both* gasdynamics and chemical reaction kinetics occur in an interactive manner in a very short time.

It has been only in the past two decades or so that research in the field of explosion phenomena has made substantial progress, largely due to advances in fast-response solid-state instrumentation for diagnostic experimentation and high-capacity electronic digital computers for carrying out complex theoretical studies. As the pace of such explosion research quickened, it became evident to research scientists on a broad international scale that it would be desirable to hold a regular series of international conferences devoted specifically to this aspect of combustion science (which might equally be called a special aspect of fluid-mechanical science). As the series continued to develop over the years, the topics included such special phenomena as liquid- and solid-phase explosions, initiation and ignition, nonequilibrium processes, turbulence effects, propagation of explosive waves, the detailed gasdynamic structure of detonation waves, and so on. These topics, as well as others, are included in the present two volumes. Volume 75, *Gasdynamics of Detonations and Explosions*, covers wall and confinement effects, liquid- and solid-phase phenomena, and cellular structure of detonations; Volume 76, *Combustion in Reactive Systems*, covers nonequilibrium processes, ignition, turbulence, propagation phenomena, and detailed kinetic modeling. The two volumes are recommended to the attention not only of combustion scientists in general but also to those concerned with the evolving interdisciplinary field of reactive gasdynamics.

Volume 75—468 pp., 6 × 9, illus., \$30.00 Mem., \$45.00 List
Volume 76—688 pp., 6 × 9, illus., \$30.00 Mem., \$45.00 List
Set—\$60.00 Mem., \$75.00 List

TO ORDER WRITE: Publications Dept., AIAA, 1290 Avenue of the Americas, New York, N. Y. 10104